

C. HUTIN (author) and G. CATTEAU (co-author)

S O P E M E A

Vélizy-Villacoublay, France

-----

Abstract

SOPEMEA is carrying out numerous modal analysis tests on the site, particularly in the aeronautic field, and for this purpose we dispose of a laboratory truck.

New computer systems have recently been set up which allowed the taking over of a new test method based on an excitation of the structure simultaneously on several points by use of uncorrelated signals.

This method, as well as the new system, have been put to trial on occasion of a test performed on a french military aircraft in February 1983.

The purpose of the present paper is to :

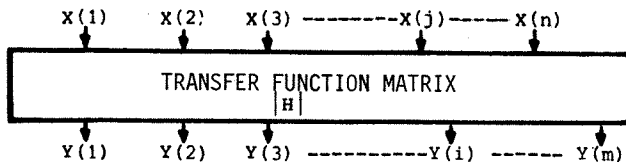
- . introduce the multi-input excitation method and system;
- . describe the ground vibration test;
- . present the results obtained and the conclusions which were drawn from them.

1. Overall presentation of the method

The technique used up to now for the ground vibration tests consisted in isolating every mode by appropriation of the excitation forces.

Since three years, and in order to reduce the immobilisation time of the aircraft, a new multi-frequency and multi-point method has been developed.

The basic principle of this method can be shortly resumed.



We shall consider the case of n inputs and m measurements.

$$Y(i) = \sum_{j=1}^n H(i,j) \cdot X(j)$$

Y(i) : spectrum of measurement i

X(j) : spectrum of input j

H (i,j) : transfer function between the points i and j

To take into account the whole of data, this equation shall be written in the form of a matrix.

$$|GYX| = |H| \cdot |GXX|$$

where : |GYX| = matrix of order m x n  
 = matrix of cross-spectra between outputs and inputs

GYX (i,j) = cross-spectrum between output i and input j

|GXX| = matrix of order n x n  
 = matrix of input cross-spectra

GXX (i,j) = cross-spectrum between input i and input j

|H| = matrix of order m x n  
 = matrix of transfer functions

The determination of this matrix is therefore given as follows :

$$|H| = |GYX| \cdot |GXX|^{-1}$$

This equation may be used as far as the matrix of input cross-spectra can be inverted, i.e. if it does not present any singularities. (Input spectrum equal to zero at a given frequency, non-independent inputs).

The curve fitting of the transfer functions thus obtained allows to develop the modal characteristics. The advantages of this method are mainly :

- . reduction of number of excitation configurations, which results in reducing the test time.
- . better distribution of energy and therefore better accuracy of measurements, and better linear estimation of a system in front of non-linearities.
- . consistency of measurements : when each column of the matrix is measured independently there may be some shifts in frequency due to behavior variations of the structure. The multi-point excitation allows to remove these errors. It becomes possible to compare the measurements of one column with measurements

of another and to make linear combinations between them in order to reduce modal density. This may be taken as a sort of mathematical appropriation.

## 2. Description of the system

The system allowing to use this method has been chosen in order to meet three requirements :

- . processing capacity of a great number of data (256 measurement points, 6 to 8 excitation points)
- . high processing speed in order to deliver results on the site
- . accuracy of results in order to use them for flutter calculation.

The structure of the system is shown on figure n°1.

The system is organized around two processors :

- . one mini-computer (CII HB MINI 6/43)

The function of this processor is to control the peripherals and to hold a dialogue with the user.

- . one array processor (FPS 100)

This processor with parallel structure is particularly well suited to all calculations of iterative type and especially to signal processing (for instance, FFT 1024 points calculated in 4 ms).

Standard peripherals are connected to the mini-computer :

- . disc unit (80 Mb) for the storage of programs and processed data
- . magnetic tape unit : 1600 BPI - 45 ips
- . graphic display + hardcopy (TEKTRONIX 4114)

It enables user dialogue, visualization of results and animated display.

- . one plotter is used for the plotting of mode shapes.

Two peripherals are connected with the array processor by means of two GPIOP (General Programmable I/O Processor) :

- . one 128-channel data acquisition system developed by SOPEMEA

Every one of these channels is fitted with a programmable filter and with a sample and hold unit. The frequency of acquisition may be higher than 400 words/s.

- . one disc of 80 Mb allowing the storage of acquisitions at a rate of 400 k-words/s.

Every GPIOP interface is programmable independently of the array processor. One may, therefore, perform simultaneously four functions :

- . data acquisition through GPIOP n° 1
- . storage of acquisitions on disc through GPIOP n° 2
- . various calculations by array processor
- . output of results by the mini-computer.

The algorithm implanted for the estimation of modal parameters is known as POLY-REFERENCE ALGORITHM.

It develops a technique similar to the one of the

least square complex algorithm, but offers supplementary advantages thanks to the consistency of measurements.

A matrix is generated on the basis of the whole set of measurements (with the whole matrix of transfer functions), and for a maximum number of degrees of freedom (MAXDOF).

The poles are systematically calculated for all values of NDOF (Number of Degrees of Freedom) up to MAXDOF.

One visualizes then on the graphic display a synthesis of the results, showing clearly the evolution of poles according to the number of degrees of freedom.

The value of the most stable pole is then selected by the software for each identified mode (see figure n° 2).

The calculation of residues is performed in the frequency domain for each column of the matrix  $|H|$  and a single estimation of the modal vector is made by means of the "MODAL ASSURANCE CRITERION" selecting among modal vectors.

## 3. Use of the method

In order to check the algorithm implanted on our new system, several tests of modal analysis have been performed over different aircrafts and more particularly over a MIRAGE F 1 plane bearing external stores, in February 1983.

This test was carried out using two methods :

- . multiple excitation with input of uncorrelated signals used in different configurations
- . standard method used since about twenty years by SOPEMEA in the aeronautic field, and which lies in isolating the modes one by one with help of different combinations of sine excitations.

This process, which has been successfully used in a great number of aircraft tests, is a good reference for the interpretation of results and the validation of the new method.

### 3.1. Test description

#### 3.1.1. Test setup

##### Suspension

The aircraft was suspended at about 1,5 Hz by means of three pneumatic devices placed under the structure.

##### Excitation

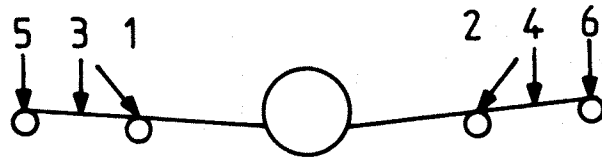
One generator manufactured by SOPEMEA is able to deliver up to 6 uncorrelated random signals.

Each output of this generator is filtered by means of a KROHN-HITE pass-band filter with a cut-off slope of 48 dB/octave.

figure 3

The filtered signals are dispatched to several electrodynamic amplifier plus exciter facilities whose main features are as follows :

- . maximum force : 200 N
- . stiffness imposed to the structure : 5950 N/m
- . mass of moving element : 365 g
- . frequency range : 0 to 200 Hz
- . power amplifier : 160 W with high feedback delivering a current which is proportional to control voltage without phase displacement and which ensures a constant level of force whichever may be the reaction of the structure.
- . possibility of regulation of force level.
- . exciter suspended to a crane at 1 Hz.



The conditions of acquisition were as follows :

- . sample frequency for each channel : 100 Hz
- . cut-off frequency of anti-aliasing filters : 30 Hz
- . acquisition of 64 measurement channels during about 40 minutes to dispose of 53 elementary averages i.e. 105 averages for an overlapping coefficient of 50 %.

### Measures

The responses of the structure are measured by means of WILCOXON piezoelectric accelerometers fitted with load amplifiers together with an incorporated integrator delivering the velocity signal.

The signals are dispatched to a multiplexer whose channels are fitted each with one sample and hold unit and one anti-aliasing filter.

#### 3.1.2. Excitation configurations

In order to investigate in the best conditions all natural modes of the aircraft bearing stores under the flying surface, we were led to use two excitation frequency ranges :

##### a) from 5 to 20 Hz

This low frequency range was chosen in order to study throughoutly the store modes.

Two excitation configurations were considered :

- . 4 excitation points (4 LF)
  - 2 excitations at the tips of wings following a vertical axis ( 3 and 4 )
  - 2 excitations at 45° of the vertical axis on the two stores under flying surface ( 1 and 2 )
- . 6 excitation points (6 LF)
  - the same as above
  - 2 supplementary excitations following one vertical axis on stores placed at the tips of wings ( 5 and 6 ).

##### b) from 5 to 50 Hz

This frequency range was chosen in order to investigate the natural modes of the aircraft.

Three excitation configurations were considered :

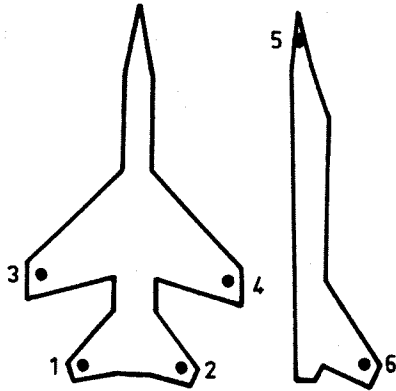
- . 4 excitation points (4 HF)
  - 2 excitations at the tips of the wings following one vertical axis ( 3 and 4 )
  - 2 excitations at the tips of horizontal tail following one vertical axis ( 1 and 2 )
- . 5 excitation points (5 HF)
  - the same as previously
  - one supplementary excitation at the front of the nose following one horizontal axis (5)
- . 6 excitation points (6 HF)
  - the same as for the second configuration
  - one supplementary excitation at the top of the vertical tail following one horizontal axis (6)

(see figure 4)

The conditions of acquisition were as follows :

- . sample frequency for each channel : 200 Hz
- . cut-off frequency of anti-aliasing filters : 60 Hz
- . acquisition of 96 measurement channels during about 20 minutes to dispose of 53 elementary averages, i.e. 105 averages for an overlapping coefficient of 50 %. It has to be noted that the place of accelerometers was not the same as for low frequency tests, particularly at the

figure 4



level of stores. In both cases the acquisitions were carried out without discontinuity in order to have the possibility of ZOOM.

### 3.1.3. Data processing

All processings were made with help of the software previously presented for every one of the five test configurations :

- . demultiplexing of data and storage on disc connected with array processor
- . definition of test parameters
- . calculation of input cross-spectra
- . calculation of input-output cross-spectra
- . inversion of input cross-spectra matrix
- . calculation of complete transfer function matrix
- . storage of transfer functions on the disc connected with array processor
- . visualization of these functions, and plotting
- . calculation of transfer function poles by use of the "POLY-REFERENCE ALGORITHM" for a number of degrees of freedom from 1 to 60
- . automatic sort of poles and printing of a listing of retained modes, listed by order of validity.

Every one is characterized by frequency and damping values. The corresponding number of degrees of freedom is selected as giving the most stable values and according to a quality coefficient.

- . calculation of residues in the frequency domain.
- . visualization and plotting of transfer functions measured and curve-fitted.
- . calculation of natural shapes, animated display and plotting.

## 4. Presentation of some results

### 4.1. Calculation of transfer functions

Some transfer function curves are given : figures 5, 6, 7.

To bring into evidence the quality of measurements obtained, we present the response of one point located on a wing tip store, at one place where measurement might have been inaccurate (rattle problems, non-linearities a.s.o.).

The functions obtained in the five excitation cases (4 LF, 6 LF, 4 HF, 5 HF, 6 HF) are gathered in order to bring into notice the consistency of all these results.

It can be noted that these functions are not very much noisy and that the augmentation of number of excitators does not involve a diminution of the quality of curves.

Some noisy areas appear whenever an excitation is induced perpendicularly to the measurement axis, but only for low levels.

It can be specified that curves delivered for a growing number of excitators are superimposable.

### 4.2. Calculation of poles

The results are gathered in following synoptic table (figure n°8).

figure 8

Mode number	VALUE	EXCITATION					
		appropriated	4 BF	6 BF	4 HF	5 HF	6 HF
108	Frequency (Hz)	4,85	4,89	4,94	4,90	4,90	4,89
	Damping (Z)	0,49	0,44	0,66	0,57	0,51	0,60
101	F	6,93	7,01	7,01	7,01	7,00	6,99
	D	0,73	0,73	0,83	0,66	0,77	0,78
102	F	7,41	7,66	7,66	7,66	7,66	7,64
	D	1,21	0,81	0,96	0,87	0,92	0,93
103	F	7,48	7,75	7,78	7,74	7,73	7,72
	D	1,35	0,97	1,23	0,95	0,97	0,97
107	F	10,10	10,28	10,28			
	D	2,2	2,42	2,41			
106	F	10,17	10,35	10,39			
	D	2,64	3,80	3,68			
109	F	11,18	11,55	11,55	11,66	11,60	11,57
	D	2,3	1,54	1,54	2,04	2,10	1,97
114	F	not measured	13,23	13,22	13,41	13,36	13,32
	D	not measured	1,16	1,25	1,37	1,34	1,33
105	F	14,40	14,55	14,49	14,66	14,67	14,62
	D	1,77	1,84	2,08	1,73	1,87	1,79
104	F	15,33	15,55	15,51	15,57	15,55	15,51
	D	1,03	0,88	0,93	0,84	0,85	0,90
121	F	not measured	16,41	16,38	16,47	16,41	16,40
	D	not measured	0,91	0,93	0,90	1,09	0,95
130	F	not measured			19,54		19,61
	D	not measured			3,15		2,86
119	F	not measured			21,54	21,58	21,45
	D	not measured			3,58	3,61	3,24
118	F	not measured			22,06	22,07	21,86
	D	not measured			3,73	3,53	3,70

The study of this table leads to following remarks :

#### a) Mode identification

The test with appropriation being partial, some modes were therefore not measured.

However, results of another test on this same plane allowed to check that the supplementary modes found by multi-input excitation were correct. Modes 107 and 106 were not found by means of excitations 4 HF, 5 HF and 6 HF, as these are store modes. The only one anomaly concerns the mode 130, which was not found in the case of 5 HF. Modes located higher than 25 Hz could not be identified because of a lack of accelerometers on tail and fuselage.

b) Values found for the poles

The values found for the poles (frequency plus damping) in 5 cases of multiple excitation are very consistent. Some differences appear in the cases of modes very closely concerned with one type of excitation, particularly in the case of store modes. The greatest differences were found between the test with appropriation and the test with multiple excitation.

. Frequency :

Maximum divergence of 4,3 % for the mode 109 (fuselage mode).

This divergence originates from the lack of accelerometers on the fuselage in the case of multiple excitation.

. Damping :

Maximum divergence of 44 % for the mode 106 (store mode).

This fact may be explained by the consideration that forces introduced are much more important in the case of appropriated excitation. The non-linearities of the aircraft are estimated by plotting impedance curves giving the evolution of the natural frequency and of the damping according to the global level of introduced forces. It can be specified that investigation of these curves completely explained all the discrepancies which were found.

4.3. Calculation of natural shapes

Natural shapes corresponding to the poles of the table shown on § 4.2., were plotted in the five excitation configurations as well as for the standard test. We cannot include a great number of curves in this paper, therefore we shall choose 4 modes whose shapes as found for 4 HF, 5 HF, 6 HF and the appropriation test, are gathered on figures 9 and 10 (at the end of this paper).

Each shape is plotted on two draft pictures of the aircraft.

- . the top view (axes X and Z) represents mode shapes following axis Y
- . the bottom view (axes X and Y) represents mode shapes following axis Z
- . the mode shapes of stores are to be found outside of the aircraft draft for a better comprehension.
- . noddle lines are represented by a dotted line.

Thus can be checked the high level of consistency of the different results.

5. Conclusion

Results obtained are coherent and confirmed by the standard ground vibration test.

Our new system with array processor allows the use of multi-input excitation method for aircraft tests on the site, in which case the data processing has to be accurate and fast.

The growing number of excitations, up to 6, does not involve a loss of quality of the measurements, nor any processing problem. We did not meet any numerical resolution problem related to the high number of data to be processed.

Our aim is now to use this system in a large number of test occurrences, to acquire a good experience of this method, and to apply it more and more frequently in order to benefit of its advantages.

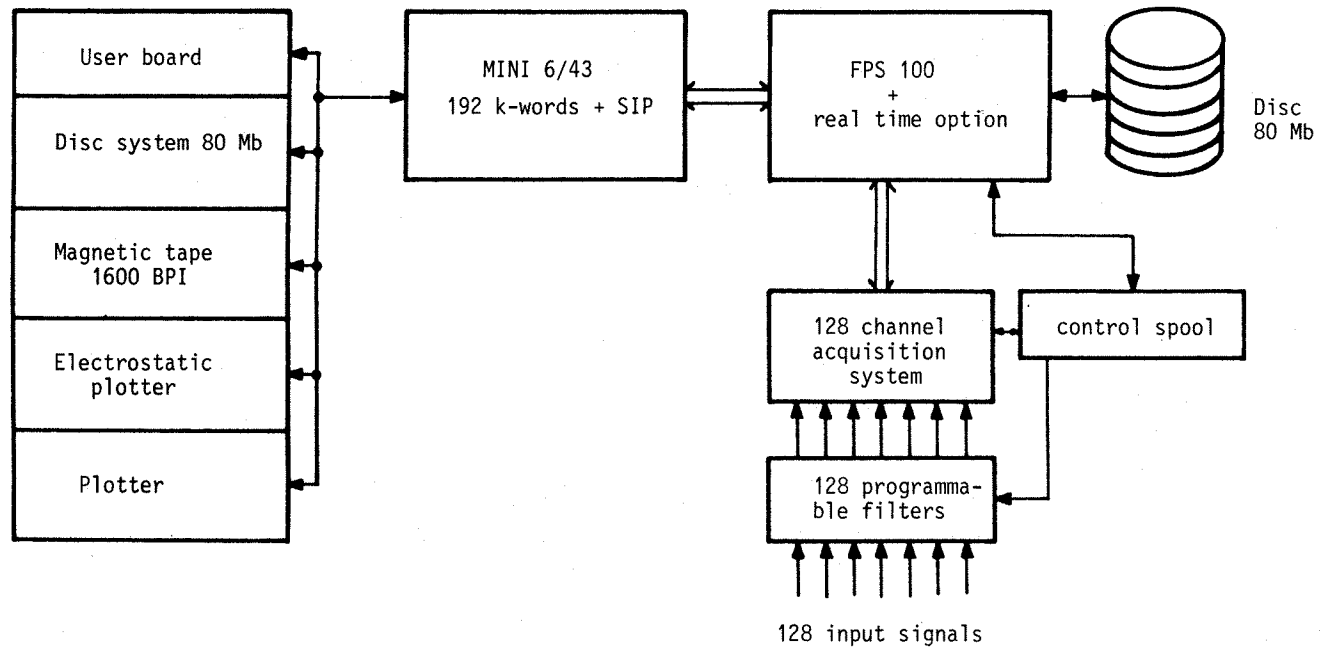
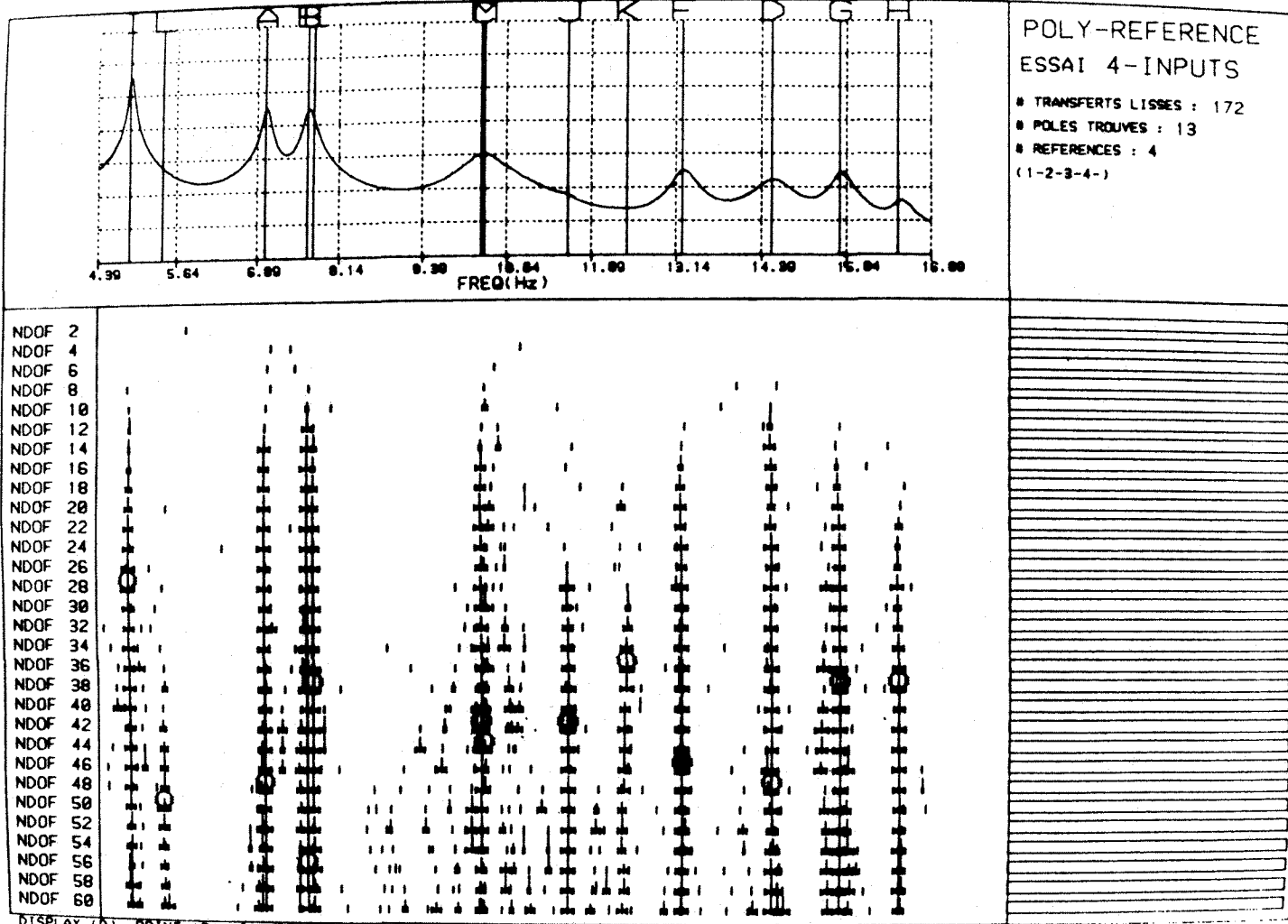
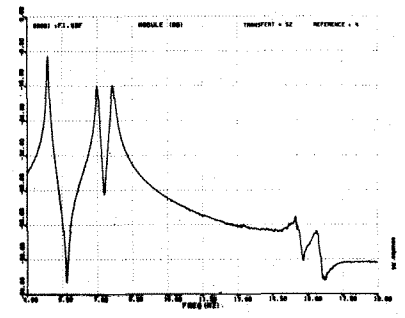
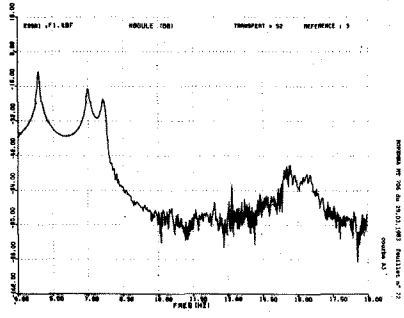
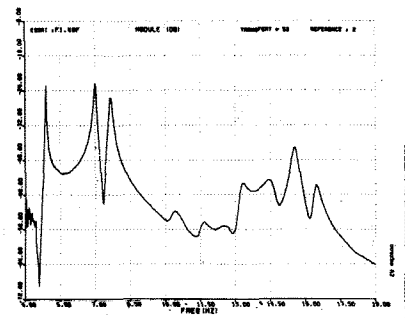
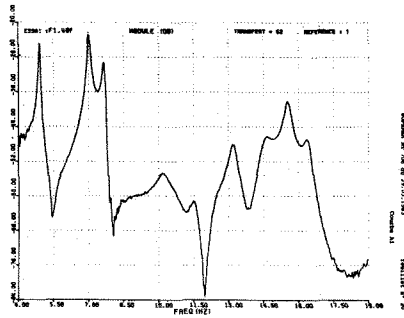


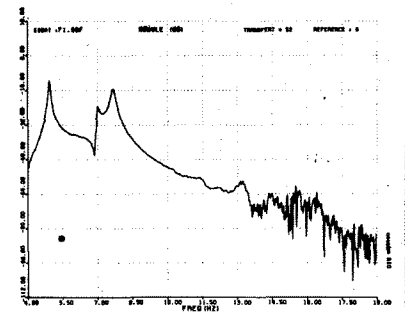
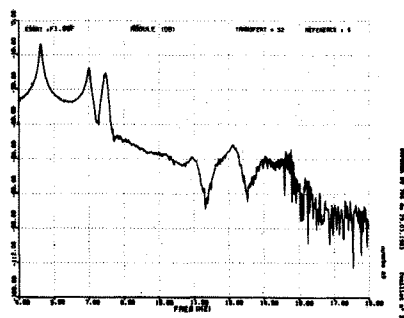
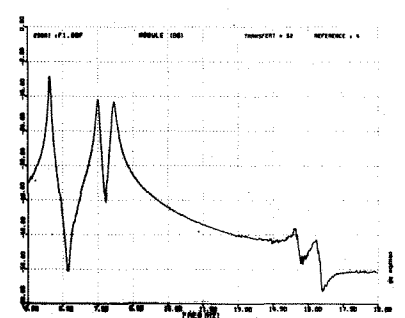
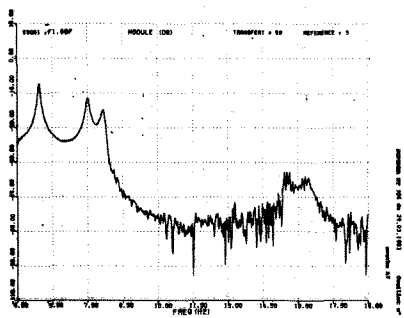
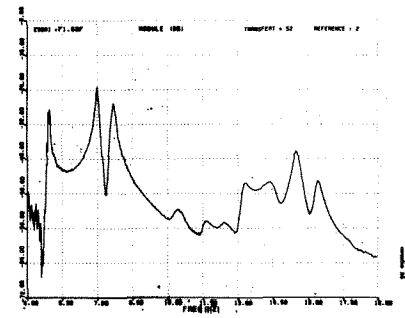
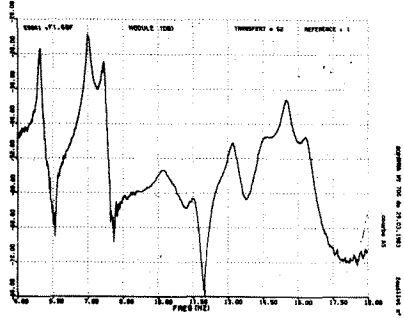
Figure n° 1

Figure 2 : Modal parameter estimation





**Figure 5**







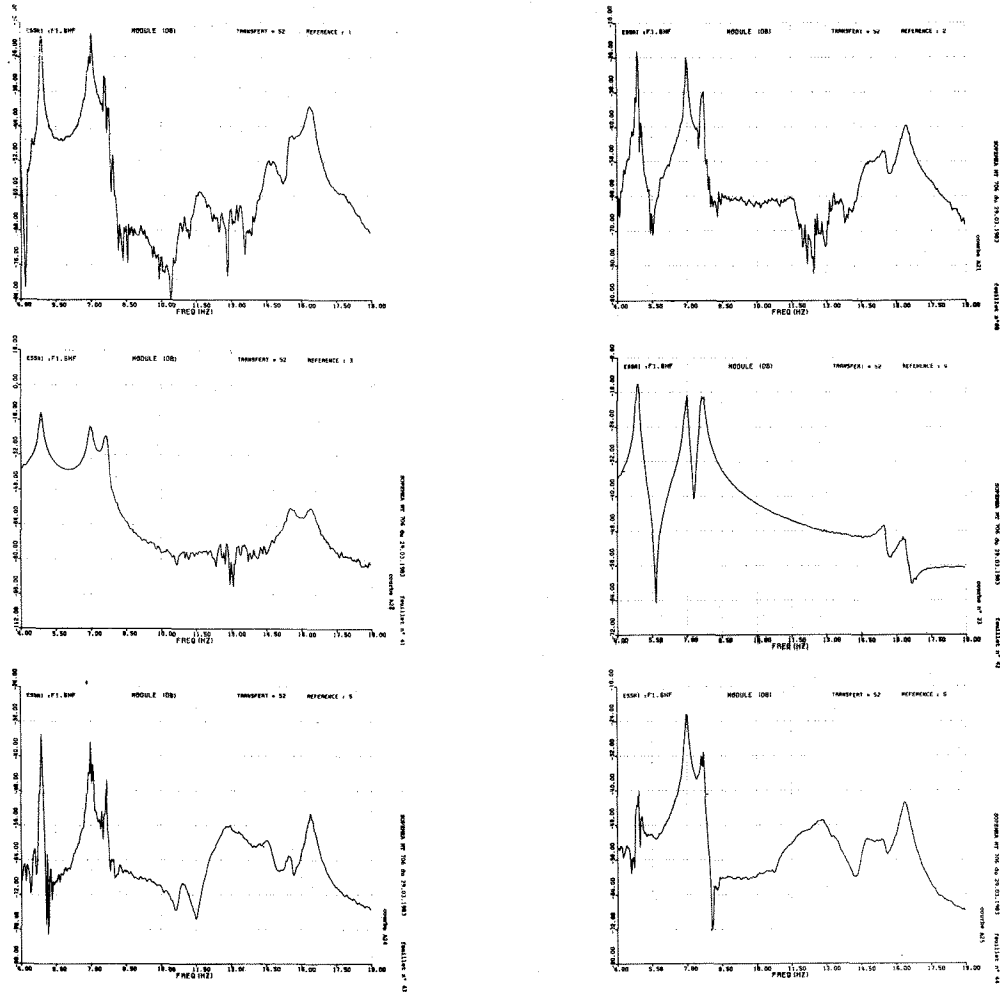


**Figure 7**

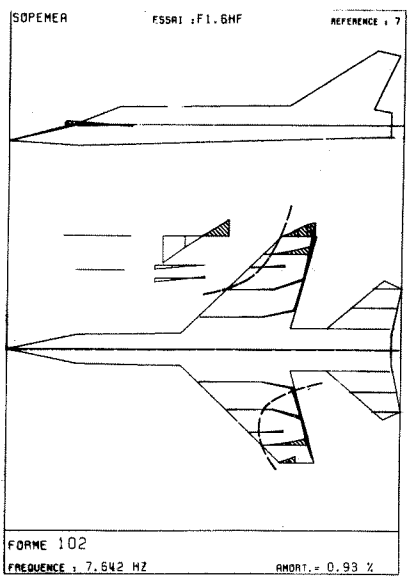
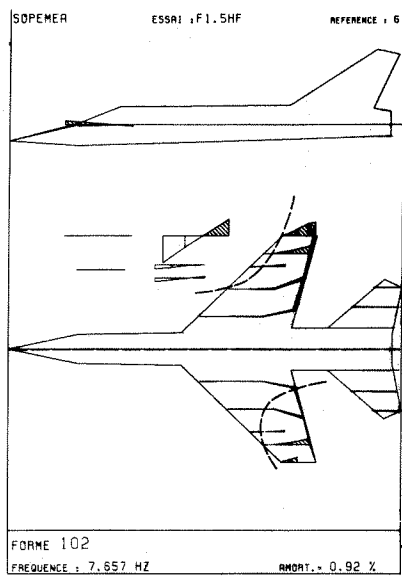
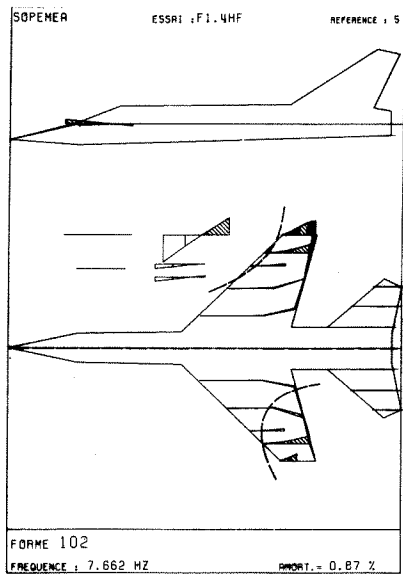
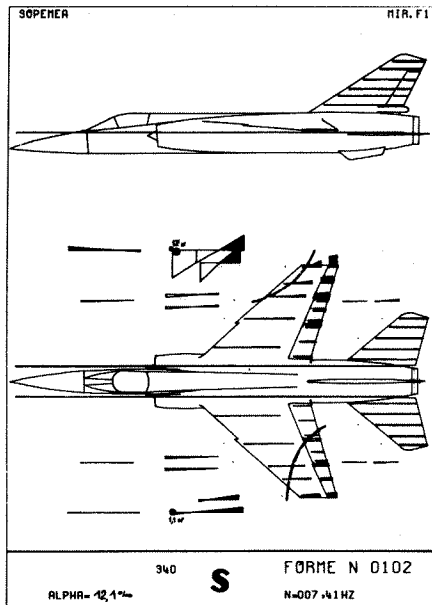
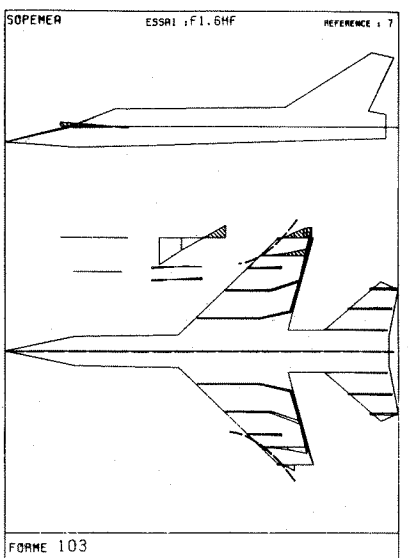
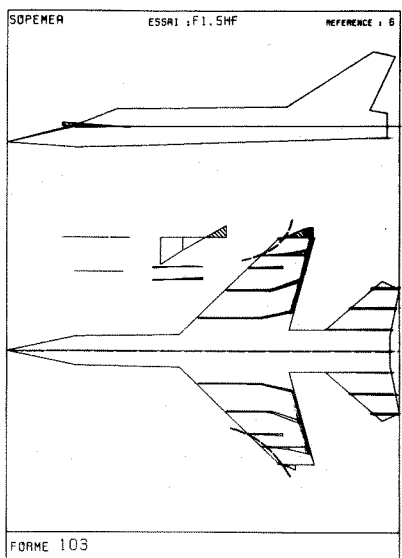
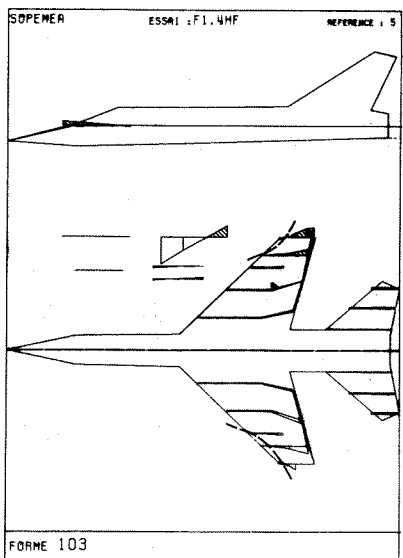
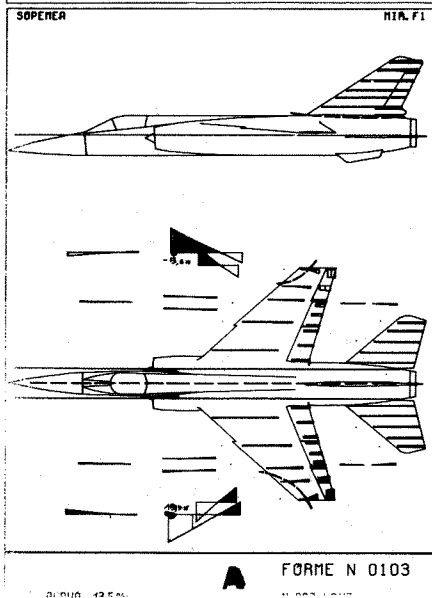


Figure 9



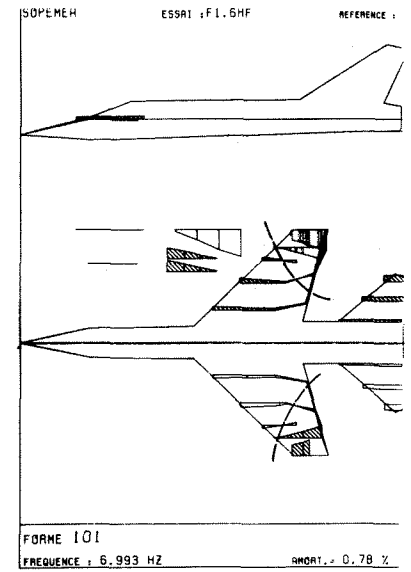
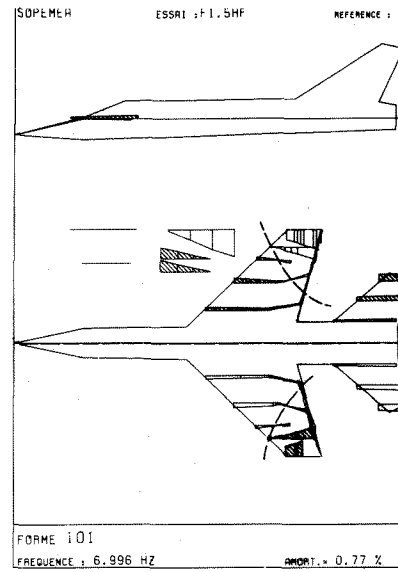
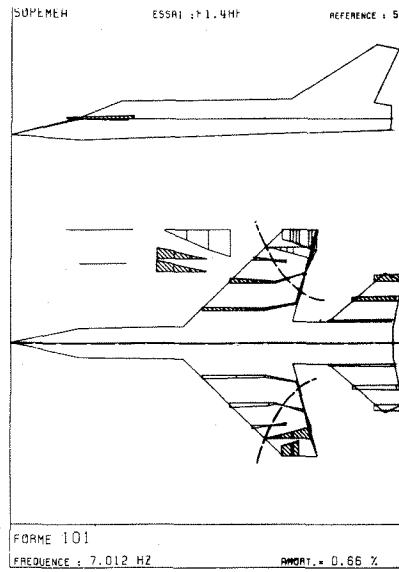
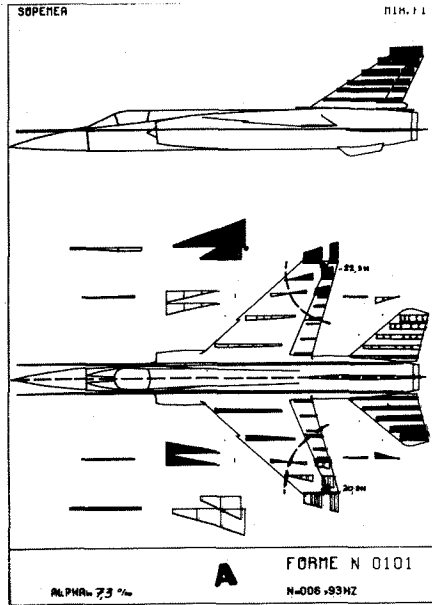
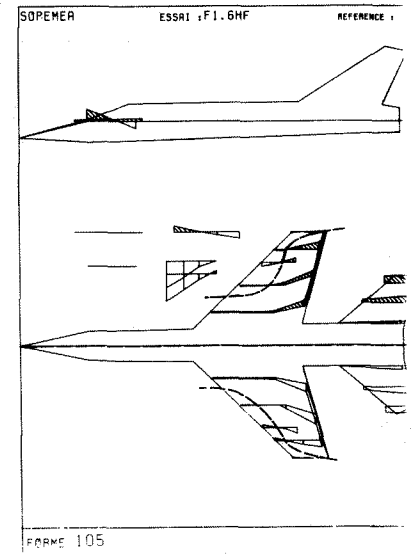
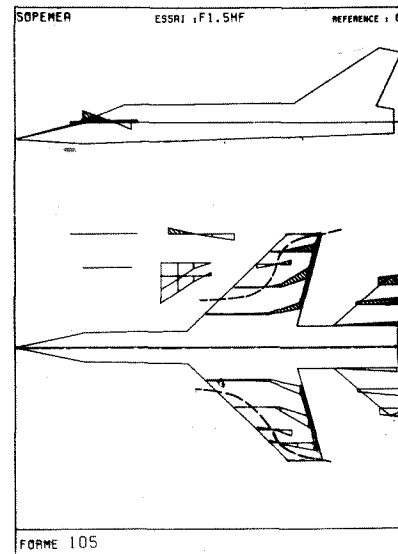
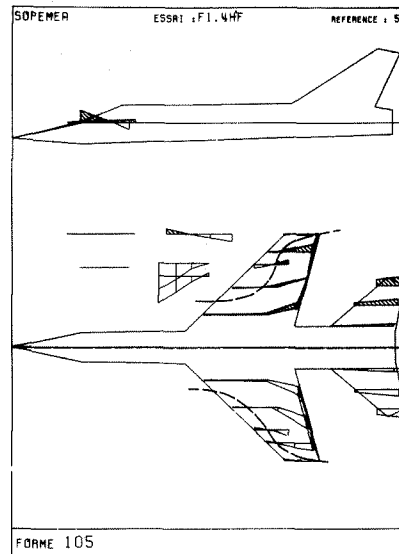
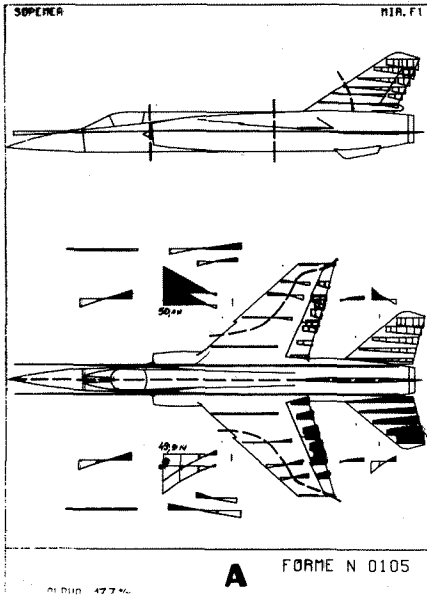


Figure 10



# Propellers in Compressible Flow

Valana L. Wells  
Stanford University  
Stanford, CA., USA

## ERRATA

POSITION	READS	SHOULD READ
p. 5, fig. 3.1	$\frac{3\pi}{2}$	$\pi$
p. 5, col. 2	4th equation	$R_n = (-1)^n \frac{-1}{n\pi} \left\{ K_{nB}(nB\rho) \int_0^\rho I_{nB}(nB\xi) d\left(\xi \frac{d\Gamma}{d\xi}\right) \right.$ $\left. + I_{nB}(nB\rho) \int_\rho^{\rho_a} K_{nB}(nB\xi) d\left(\xi \frac{d\Gamma}{d\xi}\right) \right\}$
p. 5, col. 2	5th equation	$R_n(\rho) = (-1)^n \frac{1}{n\pi} \left\{ K_{nB}(nB\rho) \int_0^\rho I'_{nB}(nB\xi) \xi \frac{d\Gamma}{d\xi} d\xi \right.$ $I_{nB}(nB\rho) \int_\rho^{\rho_a} K'_{nB}(nB\xi) \xi \frac{d\Gamma}{d\xi} d\xi$ $\left. - I_{nB}(nB\rho) K_{nB}(nB\rho_a) \rho_a \frac{d\Gamma}{d\xi} \Big _{\xi=\rho_a} \right\}$
p. 7, col. 1	eq. 3.5	$\varphi_c^\pm = \int_0^\infty A_0(\gamma) \gamma J_0(\gamma\rho) e^{\pm \frac{1}{\beta} z} d\gamma$ $+ \dots$
p.8, col. 2	eq. 4	$\rho \frac{\partial \varphi^*}{\partial z} - \frac{1}{\rho} \frac{\partial \varphi^*}{\partial \theta} + \frac{2\Gamma^*}{\rho_a \bar{c} c l_\alpha} = (1 + \rho^2) \alpha_g,$ $z \rightarrow 0, \theta \rightarrow \frac{\pi}{B}.$
p. 9, col. 1	par. 4, line 2	$\dots \Gamma^* = \sum_{k=1}^K g_k \rho^{(k+2)} (\rho_a - \rho)$